Analysis of Changes in Soil Water Content under Subsurface Drip Irrigation

Using Ground Penetrating Radar

Hirotaka Saito*[1] and Masatoshi Kitahara[2]

Abstract: In arid or semi-arid regions high-performance irrigation systems are necessary to minimize the amount of water used for agriculture purposes. Among common irrigation systems, subsurface irrigation is known to increase the water use efficiency by decreasing the water loss from the ground surface. For effective design and management of the subsurface irrigation systems, non-destructive methods to observe changes in water contents in soils are essential. Ground penetrating radar (GPR), one of the geophysical methods for subsurface measurement, has been used to observe subsurface water contents non-destructively. The main objective of this study was to investigate whether or not changes in soil water content distributions under subsurface irrigation can be observed using GPR. In this study, laboratory experiments were conducted using a soil lysimeter (120 cm × 75 cm × 60 cm) filled with river sands. An irrigation pipe was placed at a depth of 23 cm to supply water at a given head for 60 minutes. A GPR system with 1000 MHz central frequency was used in this study. GPR common offset (CO) data were collected during and after irrigation. CO profile data (radagram) show reflections from wetting fronts around the irrigation pipe. Vertical distributions of water contents at the center were then estimated from two-way travel time of EM waves. This study demonstrates that GPR can be used to observe changes in water contents due to subsurface irrigation.

Key Words: Ground penetrating radar, Infiltration, Redistribution, Subsurface irrigation, Water content

1. Introduction

Arid or semi-arid areas cover more than one third of Earth's land surface. As water resources are limited in such areas, efficient irrigation systems need to be introduced for farming. In areas where evapotranspiration rates are much greater than precipitation rates, irrigation systems supplying water directly to root zones are necessary to use limited water resources efficiently. Subsurface drip irrigation is one of such systems installed and practiced in arid and semi-arid regions (e.g., Hanson *et al.*, 1997; Kandelous and Simunek, 2010). However subsurface drip irrigation has some shortcomings that can happen frequently but are not easy to detect. For example, although irrigation pipes can be easily cracked or emitters can be readily clogged by soil particles, their exact locations cannot be easily detected unless some subsurface imaging techniques are used. To manage subsurface irrigation effectively, changes in soil moisture contents thus need to be monitored not at specific discrete locations but along subsurface irrigation pipes (in two or three dimensions).

Ground penetrating radar (GPR), one of the geophysical tools to prove subsurface, allows imaging near-surface environment non-destructively using electro-magnetic (EM) waves. GPR emits pulse EM waves from a transmitter antenna to the ground and receives the reflected or refracted waves that travel in soils at a receiver antenna. From the arrival time of the EM wave, we can estimate the EM wave velocity in the soil if the wave travel path is known. At the frequency range usually used in GPR, the EM wave velocity depends strongly on the electric property of the soil that is the relative permittivity, ε_r, as shown in Eq. (1).

$$v \cong \frac{c}{\sqrt{\varepsilon_r}} \tag{1}$$

where v is the EM wave velocity [m s^{-1}] and c is the speed of light in vacuum (3.0×10^8 [m s^{-1}]). The relative permittivity of water is about 81, while that of soil particles is about 3 to 5 and that of air is 1. This indicates that the relative permittivity of the soil is very sensitive to its moisture content (Huisman *et al.*, 2003). In fact, many studies have shown a significant and unique relationship between the relative permittivity and the moisture content (e.g., Topp *et al.*, 1980). Such empirical equations are known as petrophysical relationships.

The main objective of this was therefore to investigate the performance of GPR to monitor changes in soil moisture contents under subsurface drip irrigation.

* Corresponding Author: hiros@cc.tuat.ac.jp

3-5-8 Saiwai-cho, Fuchu, Tokyo, 183-8509 Japan

1) Institute of Agriculture, Tokyo University of Agriculture and Technology

2) Department of Agricultural and Environmental Engineering, Tokyo University of Agriculture and Technology
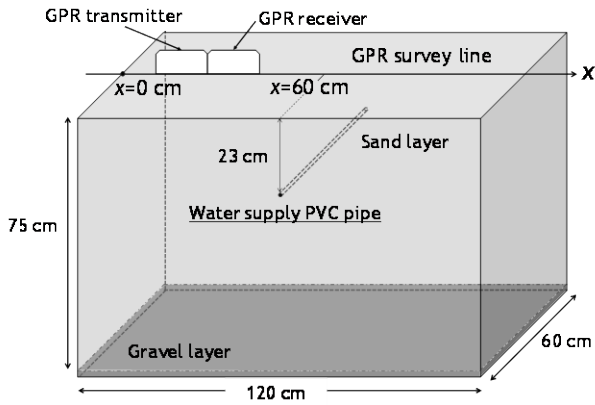
Fig. 1. Schematic diagram of the sand lysimeter.

2. Materials and Methods

In this study, a laboratory experiment was carried out using a 120 cm × 75 cm × 60 cm sand lysimeter that was made from transparent PVC (**Fig. 1**). Air dried river sand with a median particle size (d_{50}) equal to 0.34 mm was filled at a pre-determined dry bulk density of 1.55 g cm^{-3} on top of the 2-cm gravel layer at the bottom. The texture of the soil used was classified as sand from the particle size analysis.

A 2-cm diameter PVC pipe was placed horizontally at the depth of 23 cm with a 3-mm diameter water emitting inlet faced up at the middle of the lysimeter. To avoid any clogging at the inlet, a metal mesh with a diameter much smaller than the sand particle size was placed on top of the inlet before installing to the lysimeter. The PVC pipe was connected to a water reservoir tank in which a water level can be held constant. In the remainder of the manuscript, the PVC pipe is referred to as the irrigation pipe as it supplies irrigation water to the soil lysimeter. This system drawn in Figure 1 represented a subsurface irrigation system in our experiment. In this experiment, a 5-cm constant head was maintained at the water tank during 60-min irrigation. A valve at the bottom of the water tank was closed after 60 minutes to cease irrigation. The water tank was also a Mariotte bottle tank so that water supply rates could be observed.

To monitor movements of wetting fronts in the lysimeter, time-lapse common offset (CO) profiles were acquired using a surface GPR system. All measurements were carried out using a pulseEKKO PRO system (Sensors and Software, Canada) with 1000 MHz central frequency antennas. CO profile data can be acquired by keeping an antenna separation constant. In our experiment, both transmitter and receiver antennas were moved along the CO survey line (x-axis) with a fixed antenna separation of 15 cm. CO traces were acquired at every 2 cm along the survey line. After an initial profile was acquired, CO profiles were collected every 5 minutes

during irrigation. CO profiles were then collected every 60 minutes for 300 minutes after irrigation was ceased. One CO profile was finally collected at 1440 minutes.

In this study, Topp equation was used to estimate water contents from relative permittivity values as it is known to perform well with sandy soils.

3. Results and Discussion

Figure 2 shows ground penetrating radar common offset (CO) profiles acquired at 0 (initial), 20, 40, 60, 360, and 1440 minutes. The CO profile is also called "radagram" which is a collection of waveform traces recorded at all acquisition positions. The vertical axis of the profile represents the arrival time of the EM waves, while the horizontal axis represents the antenna position. Each trace has positive and negative amplitudes. Black and white colors in the radagram therefore correspond respectively to the positive end and the negative end of the amplitude range.

In the initial CO profile (**Fig. 2(a)**), there are three distinct strong signals; two parallel ones and one in a hyperbolic shape. The first parallel strong signal accounts for the pulse wave traveled directly between two antennas. This kind of wave is referred to as a direct wave. The direct wave includes waves that travel through air and along the interface of air and ground, which are called air wave and ground wave, respectively. Because the velocity of air wave is equal to the speed of light in the vacuum, an actual travel time can be calculated if the antenna separation is fixed. Then the air wave arrival time can be used to calibrate time zero of the profile data.

Another strong horizontal signal in Figure 2(a) at 9 ns is due to the reflection of the EM wave at the bottom of the lysimeter. If the moisture content of the soil is uniform inside the lysimeter, the velocity of the EM wave also becomes constant. In such a situation, reflected signals from the horizontal boundary such as the bottom of the lysimeter become horizontal. As the depth of the soil profile is constant at 75 cm in this experiment, a two-way travel time of the EM wave can be used to estimate the EM wave velocity. Once, the velocity is estimated, the average volumetric water content can be calculated from Topp equation (Topp *et al.*, 1980).

The hyperbolic shape signal peaked at $x = 60$ cm in Figure 2(a) represents a reflection of the EM wave at the irrigation pipe installed 23-cm below the soil surface at $x = 60$ cm. When a point reflection source exists, the shape of the reflected wave in the radagram becomes hyperbolic (e.g., Kearey *et al.*, 2002). In this experiment, the irrigation pipe is a point reflection source. From the hyperbolic shape signal in the radagram, the average EM velocity to the reflected point can be uniquely determined (e.g., Kearey *et al.*, 2002).
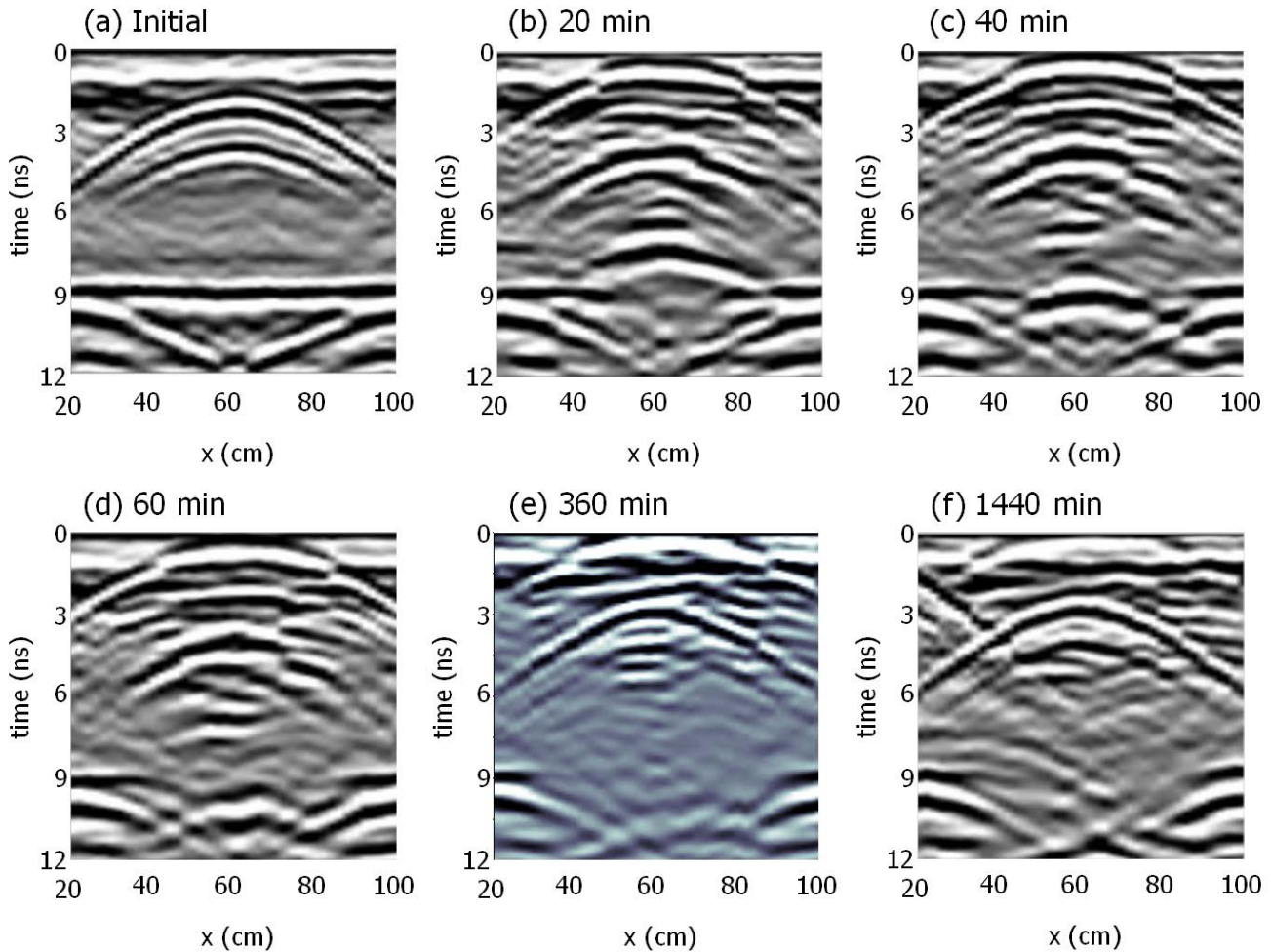
Fig. 2. Ground penetrating radar common offset profile data, radagrams, acquired at a) 0 min, b) 20 min, c) 40 min, d) 60 min, e) 360 min, and f) 1440 min (24 hr).

Figure 2(b)-(d) show respectively the CO profile obtained at 20, 40, and 60 minutes. In addition to three signals shown in Figure 2(a), a strong hyperbolic-shape reflection overlapping with the direct wave near 0 ns is observed in all three radagrams. This is due to reflection of the EM wave at the infiltration front created above the irrigation pipe, from where water was infiltrated. In Figure 2(b)-(d), there is an additional hyperbolic-shape reflection peaked respectively at 7.5 ns, 9 ns, and 10 ns. This is a reflection from the wetting front beneath the irrigation pipe. The position changes because the wetting front moves downward with time. Water infiltrated toward both above and below the irrigation pipe. Because the average EM velocity can be uniquely determined from the hyperbolic-shape signal, the depth of the reflected point, in other word, the infiltration front can be estimated.

Because the horizontal reflection from the bottom was distorted at the center in Figure 2(b)-(d), it is difficult identified the reflection from the bottom around $x = 60$ cm. However, the extent of infiltration in the horizontal direction can be easily identified. The distortion happens approximately between $x = 45$ cm and $x = 75$ cm in all three figures. This indicates that,

outside of this boundary, the soil condition is about the same as the initial condition, which means there is no water infiltrated in these areas. GPR profile data, therefore, provide not only the vertical extent of the wet area but also the horizontal extent of the wet area due to subsurface drip irrigation.

Figure 2(e) shows the CO profile at 360 minutes (300 minutes after irrigation was ceased). Although it is not clear as it is for Figure 2(b)-(d), there is still a hyperbolic shape reflection near 0 ns. This represents a reflection from the wetting front above the irrigation pipe. While the reflection at the irrigation pipe is clearly seen as others, there is no reflection observed for the bottom end of the wetting front. This may be because the wetting front beneath the irrigation pipe reached to the bottom of the profile prior to 360 minutes.

Figure 2(f) represents the CO profile obtained at 1440 minute. Since irrigation lasted only 60 minutes, this figure shows the CO profile 1380 minutes after irrigation was ceased. Due to redistribution of water, there is no clear hyperbolic-shape reflection near the surface unlike that shown in Figure 2(b)-(e). As for the reflection at the irrigation pipe, we can again see the hyperbolic shape signal clearly because it
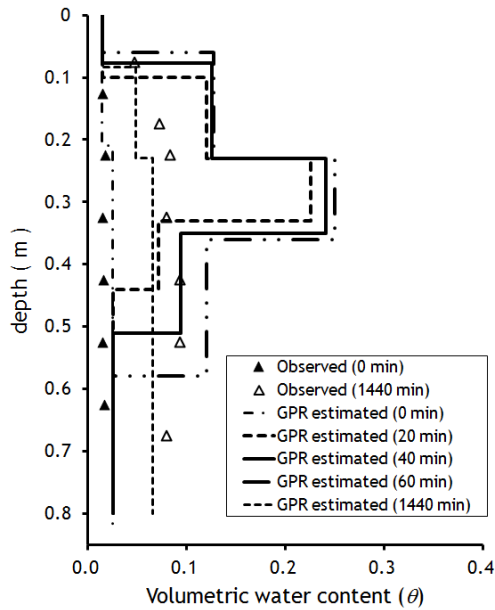
Fig. 3. **Water content distributions at *x*=60 cm obtained from GPR profile data.**

is located at the same depth even after 1440 minutes. Compare to the location of the hyperbolic-shape signal for the irrigation pipe in the initial profile (Fig. 2(a)), that is located slightly lower at 1440 minutes (Fig. 2(f)). This indicates that the average EM velocity from the surface to the irrigation pipe is lower at 1440 minutes than the initial average EM velocity to the irrigation pipe. It means that, even after redistribution of water, the water content above the irrigation pipe was still slightly greater than the initial water content. Knowing how much water left near the soil surface without disturbing soil at any given location is very critical and useful to optimize irrigation schedules in practice.

As for the reflection from the bottom of the lysimeter, there is no signal observed by 12 ns between $x = 40$ cm and $x = 80$ cm at 1440 minutes (Fig. 2(f)). It means that it took more than 12 ns for the reflected wave to be recorded at the receiver antenna. This is clearly the effect of redistribution of water where the water content beneath the irrigation pipe increased.

From the CO profiles presented in Figure 2, vertical water content distributions can be obtained at the center of the profile at $x = 60$ cm. This can be achieved by estimating the average EM velocity to the point of reflection and converting them to interval velocities. As mentioned above, for the hyperbolic shape reflection, the average EM velocity can be uniquely determined. As for the horizontal reflection, if the depth of the boundary is known, then the average EM velocity can be estimated. For all calculation, time zero was calibrated using the air wave arrival time. **Figure 3** shows water content distributions at the center of the lysimeter ($x = 60$ cm)

calculated based upon average EM velocities obtained from the CO profile data using Topp equation along with initial and final water contents directly measured by the gravitational method. As expected both GPR-based water contents and directly measured water contents for the initial condition and those at 1440 minutes match generally well and show low and uniform water content values along the center of the profile.

Water content values drastically increased around the irrigation pipe during irrigation. By converting GPR profiled data to water content distribution data, we can clearly and quantitatively obtain the vertical extent of the wet area due to subsurface drip irrigation.

4. Conclusion

This study demonstrates that ground penetrating radar (GPR) can be an effective tool to measure changes in soil water content non-destructively during subsurface drip irrigation. In our experiment, the extent of the wet area was quantitatively estimated from GPR profile data. For future work, it may be possible to inversely estimate soil hydraulic properties from changes in GPR estimated water content distributions with time.

References

Hanson B.R., Schwankl L.J., Schulbach, K.F., Pettygrove, G.S. (1997): A comparison of furrow, surface drip, and subsurface drip irrigation on lettuce yield and applied water. *Agricultural Water Management*, **33**: 139-157.

Kandelous M.M., Simunek J. (2010): Comparison of numerical, analytical, and empirical models to estimate wetting patterns for surface and subsurface drip irrigation. *Irrigation Science*, **28**: 435-444.

Huisman J.A., Hubbard S.S., Redman J.D., Annan A.P. (2003): Measuring soil water content with ground penetrating radar: A review. *Vadose Zone Journal*, **2**: 476-491.

Topp C.C., Davis J.L., Annan A.P. (1980): Electromagnetic Determination of soil water content: Measurements in coaxial transmission lines. *Water Resources Research*, **16**: 574-582.

Kearey P., Brooks M., Hill I. (2002): *An Introduction to Geophysical Exploration*. Blackwell Publishing, Oxford, U.K.